Supplement of Hydrol. Earth Syst. Sci., 25, 2199–2221, 2021
https://doi.org/10.5194/hess-25-2199-2021-supplement

Hydrology and Earth System Sciences
Open Access
EGU

Supplement of

Multivariable evaluation of land surface processes in forced and coupled modes reveals new error sources to the simulated water cycle in the IPSL (Institute Pierre Simon Laplace) climate model

Hiroki Mizuochi et al.

Correspondence to: Hiroki Mizuochi (mizuochi.hiroki@aist.go.jp)

Table S1. Pluri-annual land averages (excluding Greenland and Antarctica) of the simulated variables over the different periods used for evaluation. The chosen period does not markedly influence the observed mean, and thus the bias.

	Forced			Coupled		
	1987–2009	1993–1999	2003–2009	1987–2009	1993–1999	2003–2009
Precipitation (mm/d)	2.099	2.094	2.129	2.295	2.313	2.298
SSM (m^3/m^3)	0.163	0.164	0.162	0.194	0.193	0.192
ET (mm/d)	1.074	1.072	1.077	1.182	1.180	1.189
LAI (-)	1.555	1.550	1.571	1.470	1.457	1.492
Albedo (-)	0.212	0.211	0.210	0.222	0.221	0.220

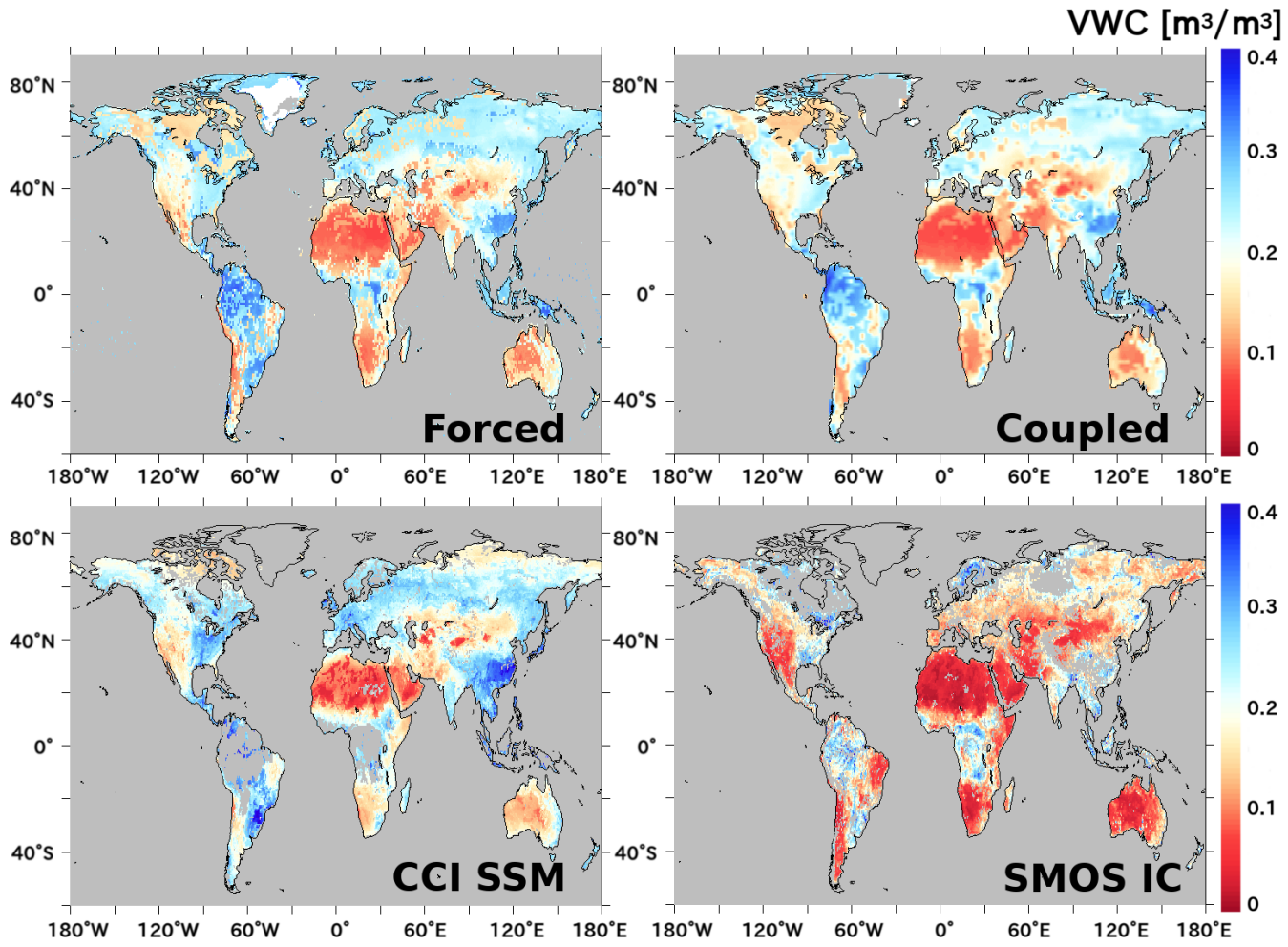

Figure S1: Pluri-annual average of surface soil moisture (SSM) in the forced and coupled mode (top row), and in the reference data (bottom row). In addition to CCI-SSM, another observation data source (SMOS-IC [Fernandez-Moran et al., 2017] version 1.05; not shown in the main text) was used just to check difference in reference data selection. All available time series data (forced: 1979–2009, coupled: 1985–2014, CCI-SSM: 1978–2018, SMOS-IC: 2010–2017) were averaged to create these maps (i.e., not separated into subperiods). The unit is SSM volumetric water content (VWC; m^3/m^3). Grey indicates null values that were excluded in the quality control process.

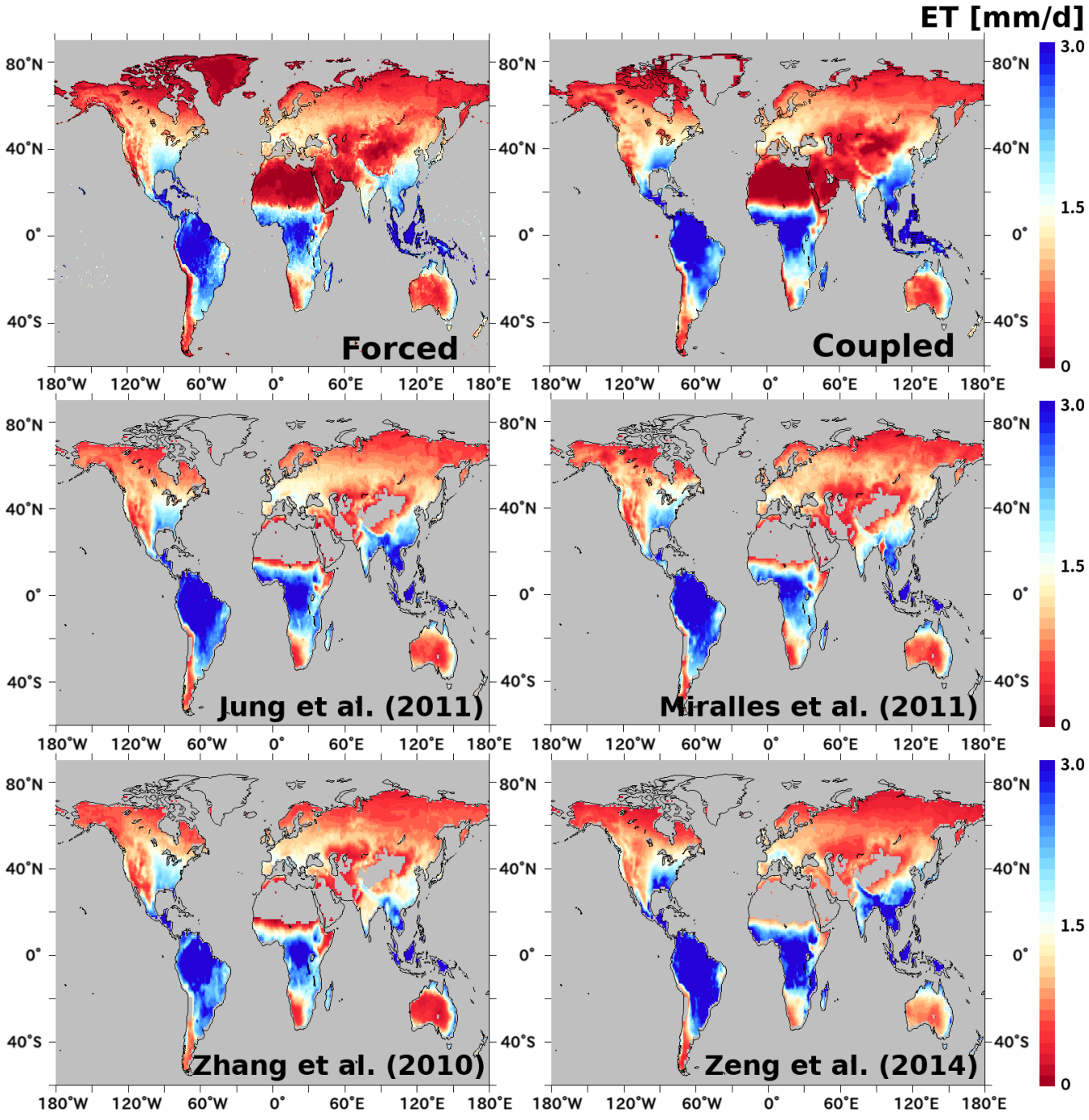

Figure S2: Pluri-annual average of evapotranspiration (ET) simulated in forced and coupled mode, and that of reference data. In addition to product by Jung et al. (2011), three other data sources (Miralles et al., 2011; Zhang et al., 2010; Zeng et al., 2014) were

checked (not shown in the main text). To take temporal average during the common duration of all reference data (1987–2006), the averaged period was slightly different from the ET study duration (1987–2009) in the main text.

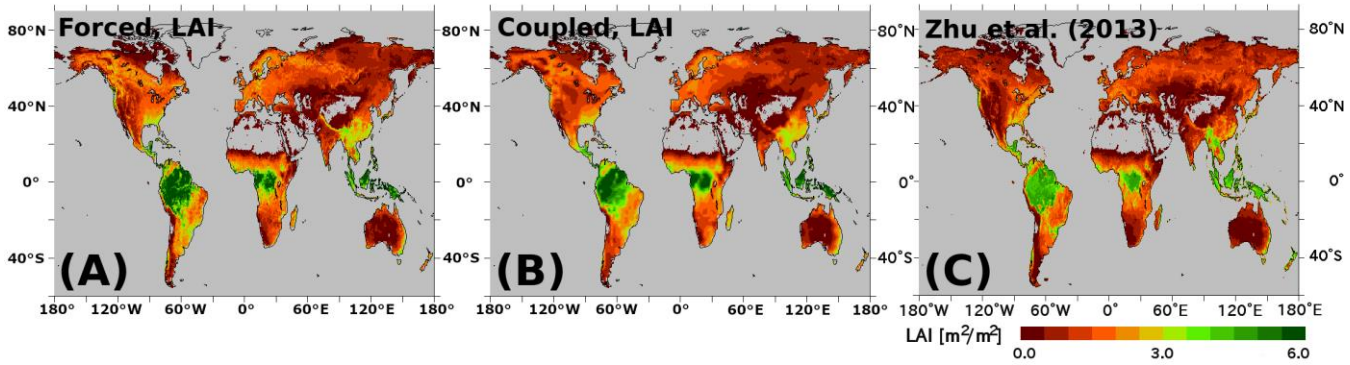

Figure S3: Pluri-annual average of LAI simulated in (A) forced mode and (B) coupled mode, and (C) the reference LAI (Zhu et al., 2013) for the study period (1987–2009).

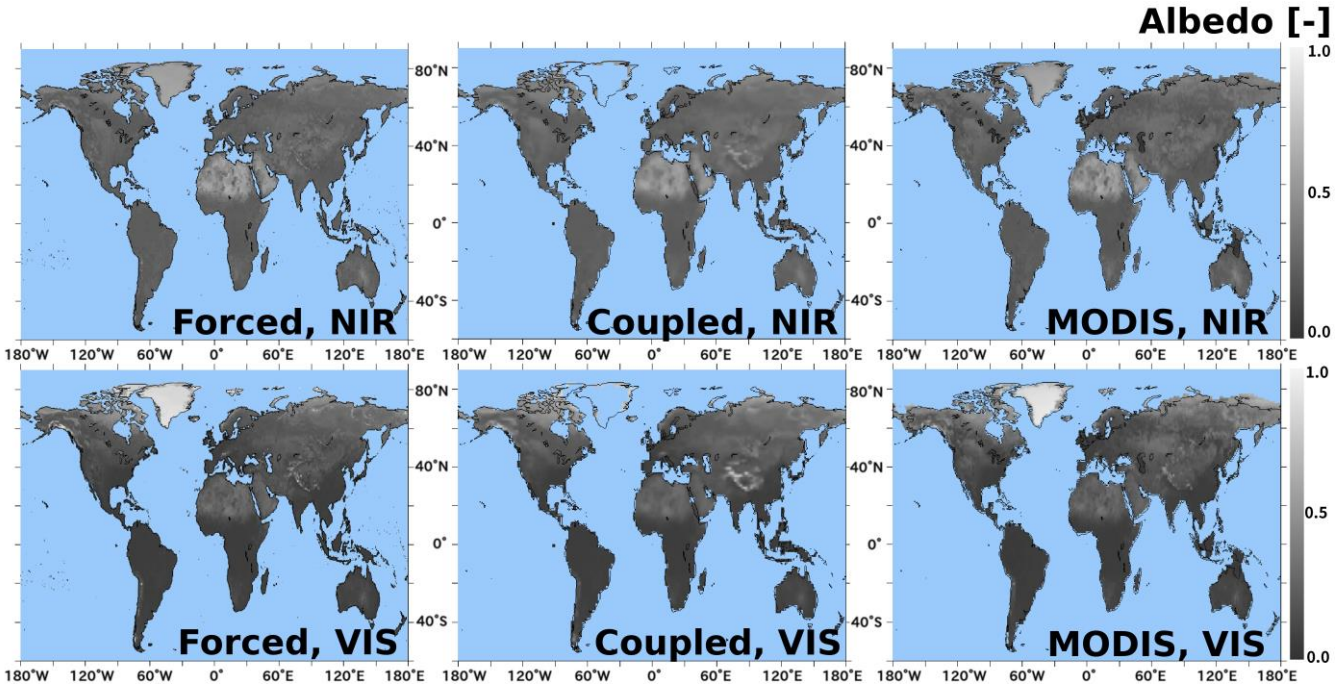

Figure S4: Pluri-annual average of albedo simulation in forced and coupled modes, and MODIS observation (Qu et al., 2014) during the study period (2003–2009), for both near infrared (NIR) and visible (VIS) spectral domains.

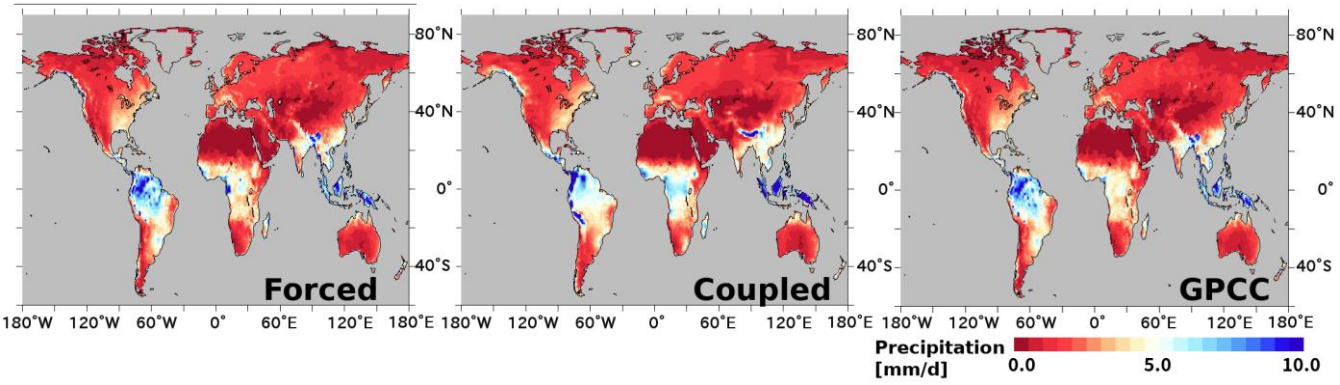

Figure S5: Pluri-annual average of precipitation in (A) forced mode and (B) coupled mode, and (C) the reference precipitation (GPCC product) during the study period (1987–2009).

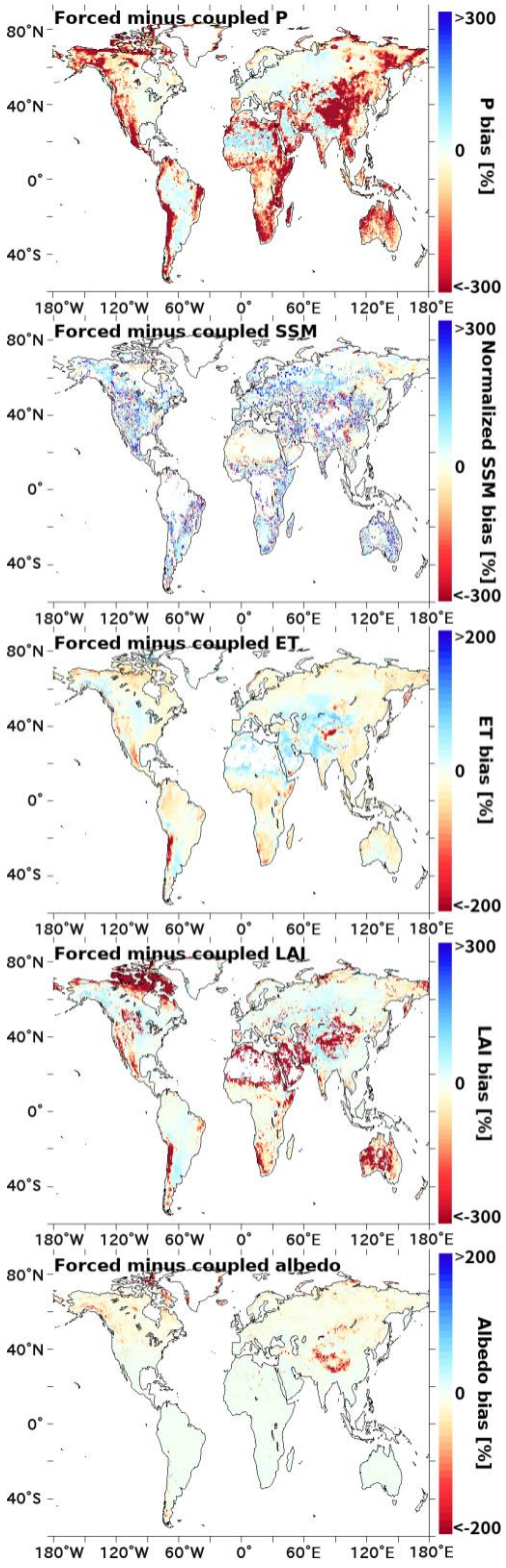
Forced minus coupled P
>300
P bias [%]
0
<-300
Forced minus coupled SSM
>300
Normalized SSM bias [%]
0
<-300
Forced minus coupled ET
>200
ET bias [%]
0
<-200
Forced minus coupled LAI
>300
LAI bias [%]
0
<-300
Forced minus coupled albedo
>200
Albedo bias [%]
0
<-200
80°N
40°N
0°
40°S
180°W 120°W 60°W 0° 60°E 120°E 180°E

Figure S6: Pluri-annual mean relative differences between forced and coupled modes for normalized SSM, ET, LAI, albedo, and precipitation, in % of the forced value. All data were temporally averaged for each study period (defined in Table 1).

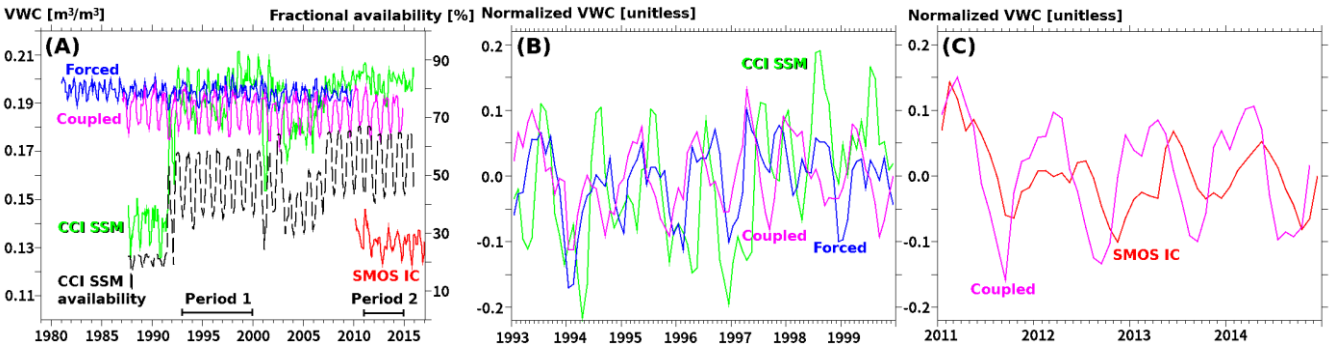

Figure S7: Time series of globally averaged SSM of forced and coupled simulations, and observations. In addition to CCI-SSM, another observation data source (SMOS-IC [Fernandez-Moran et al., 2017]; not shown in the main text) was used just to check difference in reference data selection. (A) Time series of quality-controlled data before co-masking and normalization. Dashed black line shows ratio of available pixels to all land pixels (%), which strongly affected CCI-SSM values. (B) Time series after co-masking and normalization during subperiod 1 (1993–1999), including CCI-SSM and forced and coupled simulations. (C) That during subperiod 2 (2011–2014), including SMOS-IC and coupled simulation.

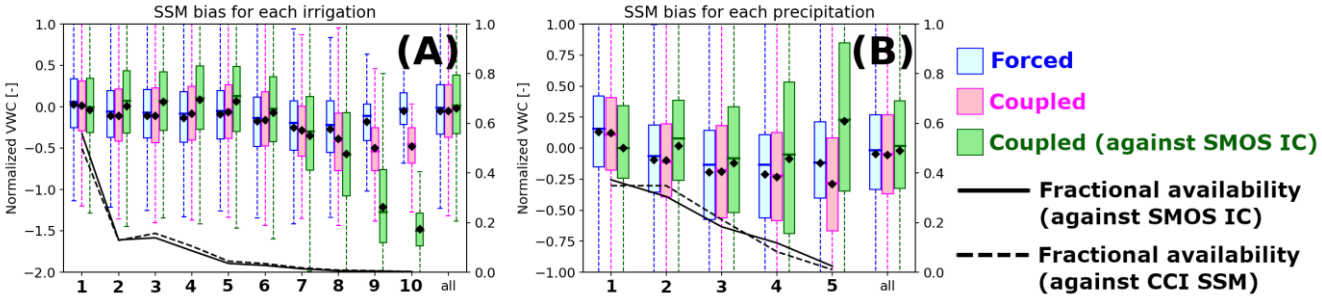

Figure S8: Different appearance in factor analysis when using different reference data (CCI-SSM vs SMOS-IC). Blue and pink boxes correspond to the mean bias of forced and coupled mode against CCI-SSM, respectively, and green boxes corresponds to the mean bias of coupled mode against SMOS-IC. The dashed and solid lines indicate pixel availability (i.e., ratio of sampled pixels to all global land pixels) for each class in CCI-SSM and SMOS-IC data, respectively. Irrigation class is defined based on the fractional coverage of irrigated area: class1 (0%), class2 (0–0.1%), class3 (0.1–1%), class4 (1–5%), class5 (5–10%), class6 (10–20%), class7 (20–35%), class8 (35–50%), class9 (50–75%), and class10 (75–100%). Precipitation class definition is the same as Table 2. Because of the different values and data coverages (particularly Amazon and Congo) between CCI-SSM and SMOS-IC, irrigation factor analysis (A) using SMOS-IC emphasized the negative bias of SSM in the coupled simulation in comparison to CCI. Precipitation factor analysis (B) emphasized the difference between the reference data that were used (CCI or SMOS), especially in the areas with extremely high precipitation (classes 4 and 5).

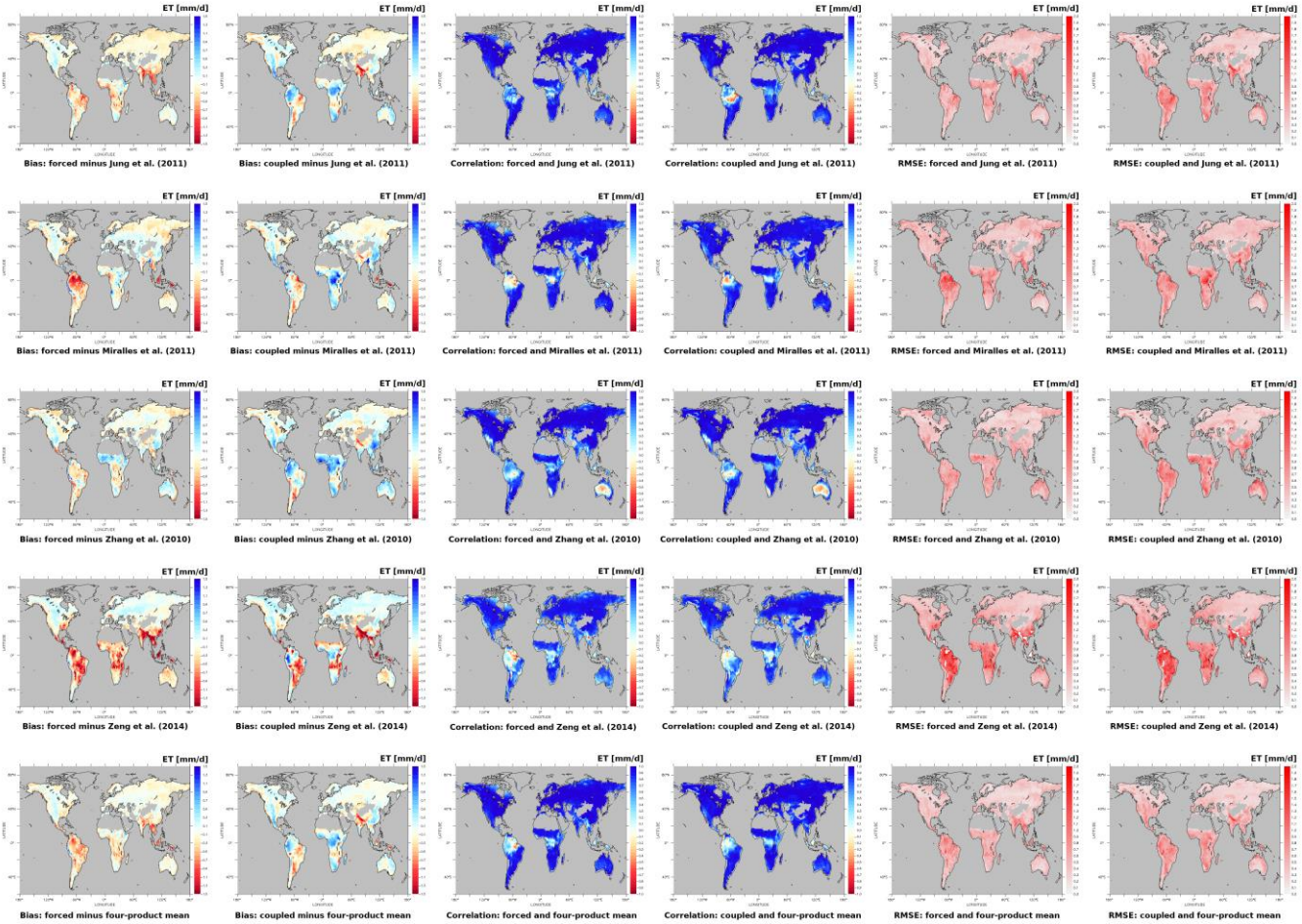

Figure S9: Mean bias, correlation coefficient, and RMSE maps derived from different reference data during 1987–2006. From the top row, Jung et al. (2011), Miralles et al. (2011), Zhang et al. (2010), Zeng et al. (2014), and the ensemble mean of those four data were used as reference. From the left column, mean bias of forced simulation, that of coupled simulation, correlation coefficient of forced simulation with each reference, that of coupled simulation, RMSE of forced simulation, and that of coupled simulation were shown. Jung et al. (2011) product has similar bias pattern as the four-product ensemble, and relatively less RMSE.